

A Comparative Study of Resonator Based Method To Estimate Permittivity

Chanchal Yadav

Department of Physics & Electronics
Rajdhani College, University of Delhi
Delhi, India

Abstract—In resonator based method, transmission line and ring resonator structures coated with the polymer film as an overlay are used to estimate the permittivity of the polymer film. The resonant frequency of the resonator depends on the guide wavelength and hence depends on the permittivity of the substrate and overlay. In this method, the permittivity is estimated by measuring the resonant frequency of the resonators. In order to improve the accuracy of the measurement, we propose a new structure which uses a sandwich substrate, which is fabricated by depositing the polymer on a grounded dielectric slab. By placing the resonator above this sandwich substrate, we are able to increase the interaction of electromagnetic fields with the polymer film, which in turn improves the sensitivity of the measurement. We demonstrate the efficacy of the method by conducting experiments and comparing the results with predictions.

Keywords—microstrip transmission line; half wave resonator; ring resonator; scattering parameter; organic polymer; permittivity

I. INTRODUCTION

Development of electronic circuits working at high frequencies, require accurate knowledge of electromagnetic properties of materials like permittivity. Resonator based methods use the concept that, the resonant frequency of an electromagnetic resonator is a function of its dimensions and properties of the material used to construct it. The resonant frequency of a transmission line based resonator depends on the length of the transmission line and the guide wavelength, which in turn depends on the permittivity of the material used to construct the line (substrate and overlay). In this paper, we compared three different structures that could be used to estimate the permittivity of organic polymer film at microwave frequencies. Sandwich substrate resonator structure is comparatively more sensitive than transmission line and ring resonator structure for same thickness of the polymer film.

Rudy et. al. [1] extended endcoupled series resonant strips technique to microstrip configurations. Bernard et. al. [2] measured the permittivity of dielectric materials by means of a microstrip ring resonator. The variational calculation of the line capacitance was used to compute the effective permittivity of the multilayer microstrip like ring resonator and the dielectric constant varies with frequency. Sumeshet. al. [3] proposed a new equation to measure the dielectric constant of materials using a microwave microstrip ring resonator at 10

GHz by empirically modifying the design equation of the effective dielectric constant of the system to account for complete and partial overlays.

In a microstrip circuit, the dielectric media above the circuit is usually air and the dielectric below the circuit is the substrate material. With air as the dielectric above the circuit, the dielectric constant ϵ_r of the substrate and the effective dielectric constant ϵ_{eff} of the microstrip are related by a filling factor that weighs the amount of the field in air and the amount of field in the dielectric substrate. In a microstrip transmission line, the electric field is concentrated between the strip and ground plane and a weak fringing field exists beyond the dielectric substrate. At the two open ends of the transmission line resonator, there are strong fringing fields which can be used in the characterization of dielectric material.

Geometry of a microstrip line resonator is shown in Fig.1. The parameters L and w represent the length and width of the resonator, respectively. The resonator is coupled to the feed line via a gap, g . Most effective way of measuring the permittivity of polymer would be to construct the microstrip line resonator on a polymer substrate. This is not a viable approach because it is not easy to deposit metal tracks on polymer films. An alternative approach could be to use the polymer as an overlay (Fig.2). If the microstrip resonator is coated with an overlay, the fringing fields will penetrate in the overlay, and thus changing the effective permittivity of the microstrip and hence the resonant frequency of the resonator. The dielectric constant of the overlay can be obtained from the change of the resonant frequency. This is the most attractive structure from the processing point of view.

Firstly the effect of coupling on the scattering parameters for a $\lambda_g/2$ long microstrip line based resonator is obtained and then the effect of changing the permittivity of the overlay on the resonant frequency of the line resonator is observed. Two more structures, a microstrip ring resonator with polymer overlay and a half wave resonator with a hybrid substrate, which is a sandwich of RT/duroid and the polymer film, are used. IE3D simulation tool is used to estimate the permittivity of the polymer film from experimentally measured resonant frequency and $|S_{12}|$.

II. MICROSTRIP RESONATOR WITH POLYMER FILM AS AN OVERLAY

In this section two types of gap coupled microstrip resonators are presented. In both cases, the polymer whose permittivity is to be estimated is introduced as an overlay. The dielectric properties of the sample are determined from the resonant properties and structural parameters of the resonator.

A. Half Wave Transmission Line Resonator

A segment of microstrip transmission line resonates when its length is approximately equal to an integral number of half wavelengths[4]. If L is the length of the line resonator (Fig.3), the relationship between the resonant frequency f and the effective dielectric constant ϵ_{eff} of the microstrip transmission line resonator is given by Eq. (1) and using Eq. (2), we can write Eq. (3) which gives the relationship between the length of the microstrip line L and the resonant wavelength λ_g .

$$\epsilon_{eff} = \left(\frac{nc}{2Lf}\right)^2 \quad (1)$$

$$\lambda_g = \frac{\lambda_0}{\sqrt{\epsilon_{eff}}} \quad (2)$$

$$L = n \left(\lambda_g/2\right) \text{ (for } n = 1,2,3,\dots) \quad (3)$$

where c is the speed of light, n is the order of resonance, the effective dielectric constant (ϵ_{eff}) is a composite of the dielectric constants above and below the line, λ_0 is the wavelength without a dielectric (free space wavelength) and λ_g is the guide wavelength (wavelength of the actual structure).

If the distance between the feed line and the resonator is large, then the coupling gaps do not affect the resonant frequency of the line resonator greatly and this type of coupling is known as weak coupling (negligibly small capacitance of the coupling gap). If the coupling is too small, very less energy is coupled into and out of the resonator which makes the measurement difficult as well as inaccurate. If the feed lines are moved closer to the resonator, however the coupling becomes tight and the gap capacitance becomes appreciable. This causes the resonant frequency of the circuit to deviate from the intrinsic resonant frequencies of the line. Hence to accurately model the line resonator, the capacitances of the coupling gaps should be considered.

Consider a weakly coupled microstrip line resonator. Since the coupling is weak, we ignore the coupling capacitance. However, due to the fringing fields at the open ends of the resonator, there exists an additional capacitance to ground. This can be taken into account in the calculation of the resonant frequency of the line by introducing an additional length, δL , at both the ends of the resonator[5]. Thus the effective length of the resonator is slightly longer than its physical length, and hence Eq. (3) is modified as Eq. (4) which gives the modified resonant condition.

$$L + 2\delta L = n \left(\lambda_g/2\right) \text{ (for } n=1,2,3,\dots) \quad (4)$$

where $2\delta L$ is the contribution due to the capacitance of the two open ends. To obtain accurate value of dielectric constant, the effect of $2\delta L$ should be taken into consideration. The parameters of microstrip transmission line resonator are listed in TABLE 1.

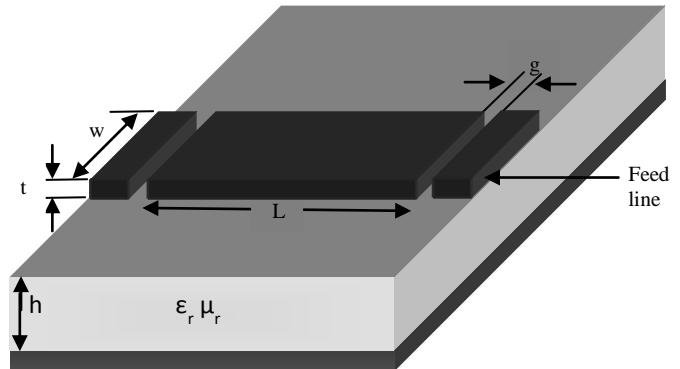


Fig.1. A microstrip line resonator with sample under test as its substrate.

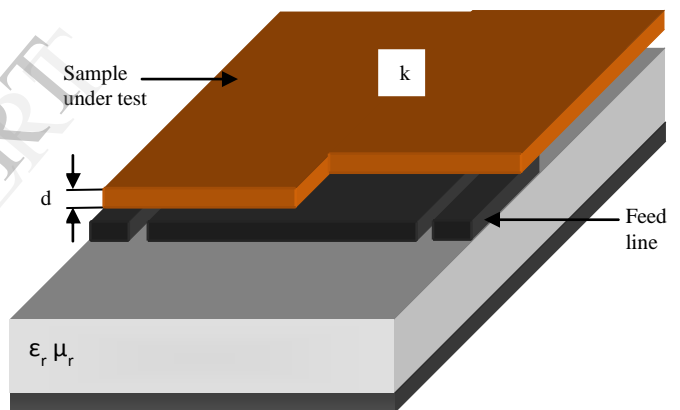


Fig.2. A microstrip line resonator with sample under test as an overlay.

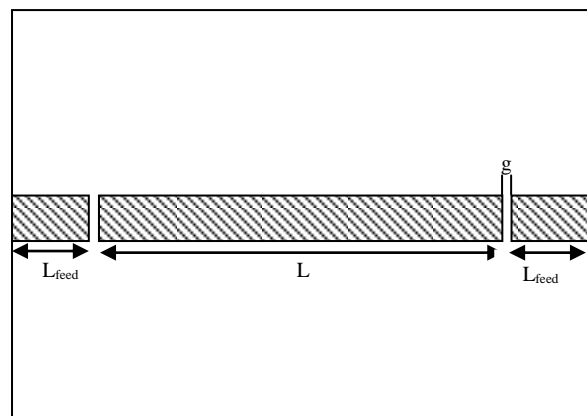


Fig.3. The sectional view of microstrip line resonator structure.

TABLE 1. LIST OF PARAMETERS OF TRANSMISSION LINE RESONATOR

Parameter	Symbol	Value
Resonant frequency	f	2.4 GHz
Length of resonator	L	45.9 mm
Length of feed line	L_{feed}	6.85 mm
Coupling gap	g	variable
Width of line	w	2.439 mm
Substrate size		60 mm x 45mm

The dielectric properties of the polymer are determined from the resonant properties and structural parameters of the microstrip line resonator. For resonator structure, we need to estimate the coupling gap. We tried different coupling gaps ($g=0.05\text{mm}$, 0.1mm , 0.2mm , 0.3mm , 0.5mm).

Fig.4 to

Fig.7 show the effect of change of coupling gap on scattering parameters for the line resonator.

As the gap between the feed line and the resonator gets larger, the reflection coefficient gets worse and the signal coupled into the other ports $|S_{12}|$ decreases. The resonance corresponds to the frequency where $|S_{11}|$ is minimum or $|S_{12}|$ is maximum. As the coupling gap decreases, interaction between the feed line and the resonator becomes stronger and hence the loading effect becomes prominent. We have used $g=0.2\text{mm}$ which is a good balance between coupling and loading.

We now consider the possibility of using this structure to determine the permittivity of the overlay. We consider two different thicknesses of overlay, and calculate the resonant frequency for different values of permittivity (κ) of the polymer film. A plot of resonant frequency versus the permittivity (κ) of the overlay (

Fig.8) indicates that as the permittivity of the overlay increases, the line resonates at lower frequency. The resonant frequency is a monotonically decreasing function of κ . The slope of this line depends on the thickness of the overlay. The response of the resonator with a thicker overlay has a large slope. For example with $10\mu\text{m}$ thick overlay we observe a change of 41 MHz in the resonant frequency, however, if the overlay is $35\mu\text{m}$ thick, the corresponding change is 102 MHz, when the permittivity changes from 1 to 9. Using a thicker overlay to estimate κ improves the accuracy of measurement.

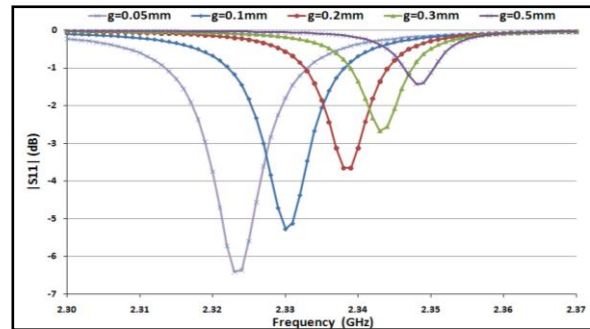


Fig.4. Magnitude of reflection coefficient of line resonator with $35\mu\text{m}$ thick overlay showing the effect of gap.

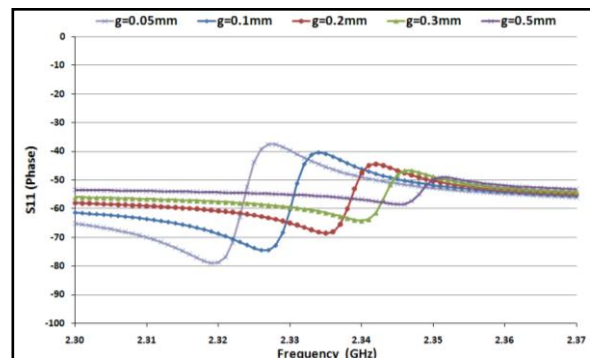


Fig.5. Phase of reflection coefficient of line resonator with $35\mu\text{m}$ thick overlay showing the effect of gap.

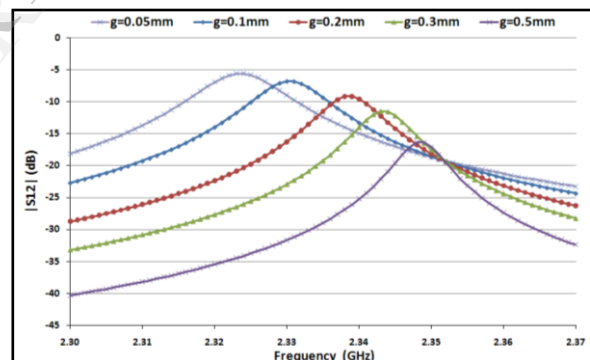


Fig.6. Magnitude of transmission coefficient of line resonator with $35\mu\text{m}$ thick overlay showing the effect of gap.

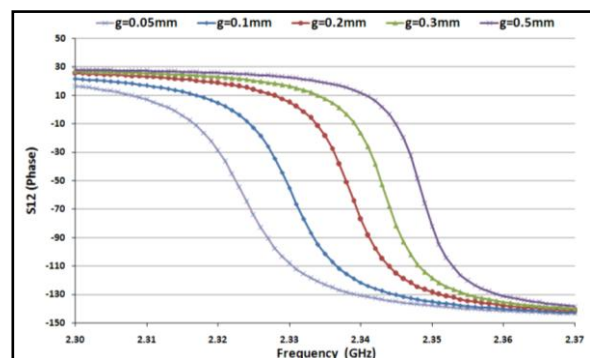


Fig.7. Phase of transmission coefficient of line resonator with $35\mu\text{m}$ thick overlay showing the effect of gap.

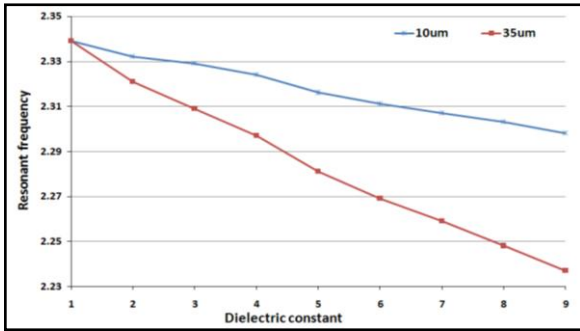


Fig.8. Resonant frequency of line resonator with overlay showing the effect of thickness.

B. Microstrip Ring Resonator

In a microstrip ring resonator, as there are no open ends so it has low radiation losses. Consider a microstrip ring resonator (Fig.9), gap coupled to two microstrip lines, located at the diametrically opposite ends. Ring resonator is merely a transmission line formed in a closed loop. The basic circuit consists of the feed lines, coupling gaps and the resonator. When the mean circumference of the ring resonator is equal to an integral multiple of a guide wavelength, resonance is established [6].

The microstrip ring resonator structure is shown in Fig.9. The frequency modes are given by Eq. (5) and hence the relationship between wavelength λ_0 at resonant frequency f_m and the effective permittivity ϵ_{eff} is given by Eq. (7) [2], [6].

$$2\pi r = m\lambda_g \text{ (for } m = 1,2,3,\dots) \tag{5}$$

$$\pi(r_1 + r_2) = m\lambda_g \tag{6}$$

$$\lambda_g = \frac{\pi(r_1 + r_2)}{m} \sqrt{\epsilon_{eff}} \tag{7}$$

$$(r_1 - r_2) = w \tag{8}$$

where r is the average radius of the ring, m is the mode number, f_m is the resonant frequencies at different orders of harmonics can be measured, and then effective permittivity of the microstrip structure can be estimated. In the calculations, we assume that the resonant frequency of the fundamental mode is known. The parameters of ring microstrip line resonator are listed in TABLE 2.

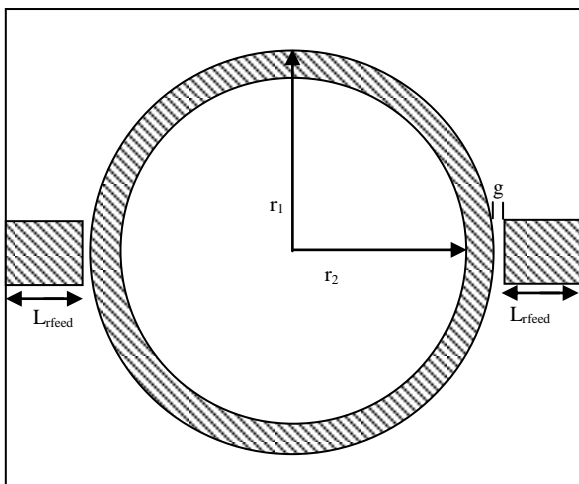


Fig.9. The sectional view of microstrip ring resonator structure.

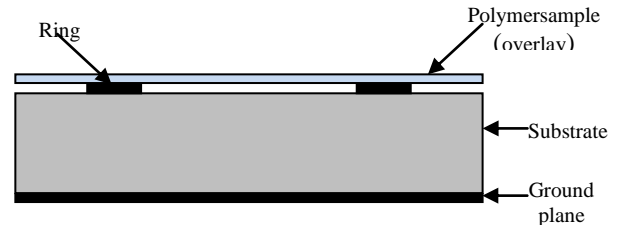


Fig.10. Microstrip ring resonator with the sample under test as an overlay.

Parameter	Symbol	Value
Resonant frequency	f	2.4 GHz
Ring inner radius	r_2	13.3909 mm
Ring outer radius	r_1	15.8299 mm
Number of segments	n	40
Length of feed line	L_{rfeed}	13.9701 mm
Coupling gap	g	0.2 mm
Width of line	w	2.439 mm
Substrate size		60 mm x 45 mm

In a ring resonator, there is no open end, so the problems due to the end effects in microstrip transmission line resonator are avoided. Usually, a ring resonator has higher quality factor than a microstrip transmission line resonator. We have used the microstrip ring resonator as a measurement fixture, and the sample under test (polymer) covers the microstrip ring resonator circuit (Fig.10).

The gap $g=0.2\text{mm}$ is chosen such that sufficient coupling ($|S_{12}| = -9\text{dB}$) is obtained. At this level of coupling, the loading is reasonably small to keep the loaded resonance frequency close to the intrinsic (unloaded) resonant frequency. Once again, we plot the resonant frequency as a function of the permittivity of the overlay for different thicknesses.

Fig.11 shows the response of ring resonator for two different thicknesses of overlay ($d=10\mu\text{m}$ and $35\mu\text{m}$).

We observe 93MHz change in frequency when the permittivity changes from 1 to 9 for $35\mu\text{m}$ thick overlay. While, for $10\mu\text{m}$ thick overlay the resonant frequency changes by 40MHz for a permittivity change from 1 to 9. So the sensitivity of resonant frequency to the change in κ is more with thicker overlay. Again, the resonant frequency is lower for thicker overlay with larger permittivity. Compared to half wave resonator, the ring resonator has a smaller sensitivity to change in permittivity

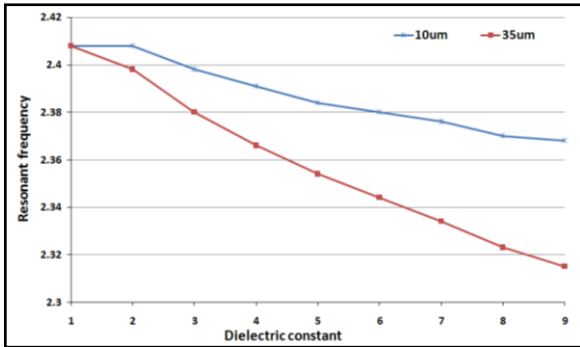


Fig.11.Resonant frequency of ring resonator with overlay showing the effect of thickness.

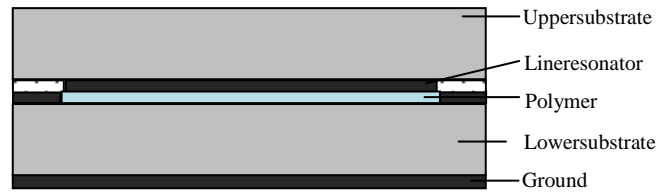


Fig.12.Cross sectional view of sandwich substrate resonator.

III. DESIGN AND ANALYSIS OF SANDWICH SUBSTRATE RESONATOR

In order to increase the interaction of fields with the polymer layer/film, a resonator is constructed on a sandwich substrate. First we take a grounded dielectric slab, on which two short length microstrip lines are etched out. On to this substrate; the polymer film is deposited using spin coating technique. The thickness of the film is measured using thickness profilometer. The resonator strip is etched out on another dielectric slab, and is placed on the polymer coated substrate such that the metal touches the polymer surface (Fig.12).

In order to remove the air gaps and ensure proper contact between the top substrate and the polymer film, petroleum jelly is used as the filling material. Permittivity of petroleum jelly is very close to that of RT/duroid substrate, and hence works as a good filling material. By applying sufficient pressure, excess petroleum jelly is taken out of the structure.

The strip width of the resonator strip is calculated from embedded microstrip line design formulae [7]. Fig.13 shows the sectional view of an embedded microstrip line where w is the width of the strip, t is the thickness of the strip, h is the height of the grounded substrate ($H = t+2*h$), ϵ_r is the relative permittivity of the substrate and Z_0 is the characteristic impedance.

Now we calculate the parameters of embedded microstrip line from substrate parameters as listed in TABLE 3 using Eq. (9) and Eq. (10).

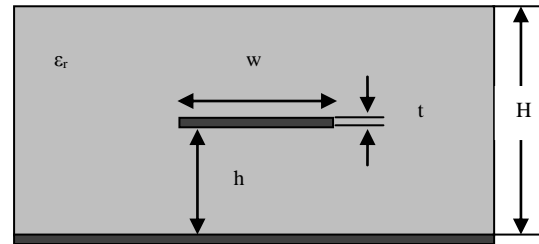


Fig.13. Sectional view of embedded microstrip line.

Cladding		(1ozED Cu/1ozED Cu)	
Lower substrate size	60mm x 45mm		
Upper substrate size	46mm x 21mm		
Feed line (Copper)	Length	L_{feed}	6.85mm
	Width	w	1.7206mm
Line resonator (Copper)	Length	L	45.9mm
	Width	w	1.7206mm
Organic polymer overlay	Dielectric constant	κ	unknown
	Thickness	d	35 μ m
Petroleum Jelly	Dielectric constant	ϵ_{rpj}	2.2
	Thickness	T	35 μ m

IV. RESULTS AND DISCUSSION

Scattering parameters are measured to estimate the permittivity of the organic polymer. Before measuring scattering parameters using vector network analyzer (VNA), we calibrate VNA using SOLT (Short-Open-Load-Thru) standard to eliminate systematic error in the system

As the terminal scattering parameters are affected by the amount of coupling between the feed line and the resonator. With sufficiently low coupling, it is possible to make the loaded resonant frequency approach the unloaded value. The amount of coupling can be controlled by introducing an offset(s) in the location of the resonator (Fig.14). For $s=0$, the

$$\epsilon_r' = \epsilon_r \left[1 - \exp\left(\frac{-1.55H}{h}\right) \right] \text{ (when } H > 1.2*h \text{)} \quad (9)$$

$$Z_0 = \frac{60}{\sqrt{\epsilon_r'}} \ln\left(\frac{5.98 * h}{0.8w + t}\right) \quad (10)$$

resonator is aligned with the feed line. The amount of coupling is decided by the gap between the feed lines and the resonator (which is 0.2mm in this case). In order to decrease the coupling, the resonator is moved away from the center of feed line (s increases). Larger offset results in weaker coupling between the feed line and the resonator. The arrangement corresponding to largest value of s gives weakest coupling.

In this study, we consider four different values of offset, viz, 0mm, 1.7mm, 4.5mm and 11mm, and study the effect of changing the permittivity (κ) of the polymer on the resonant frequency and the $|S_{12}|$ corresponding to the resonant frequency. The effect of offset and κ on the resonant frequency is shown in

Fig.15.The results shown in

Fig.16to Fig.19are obtained by EM simulations. We notice that as the permittivity increases, the resonant frequency decreases. As the offset is changed from 0mm to 1.7mm, the coupling decreases and a noticeable change in resonant frequency is observed. As the offset gets larger, the coupling gets weaker and the resonant frequency change is insignificant(

Fig.15).

Fig.16to Fig.19show the change in resonant frequency and value of $|S_{12}|$ at resonance for four different offset conditions. It is clear from these figures, the transmission coefficient decreases with larger offset.

As we perform the measurements, it is observed that, placement of the top substrate with resonator affects the measurement. In order to minimize the effect of placement on the measurement, the top substrate is placed several times and we record the resonant frequency and $|S_{12}|$ corresponding to the resonant frequency. These results are compiled as histograms and shown in

Fig.20 to

Fig.27.

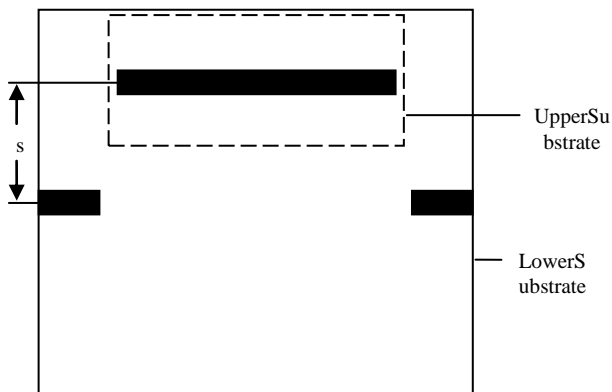


Fig.14.Sectional view of sandwich substrate resonator for resonator placed at a distance s (mm) away from centre.

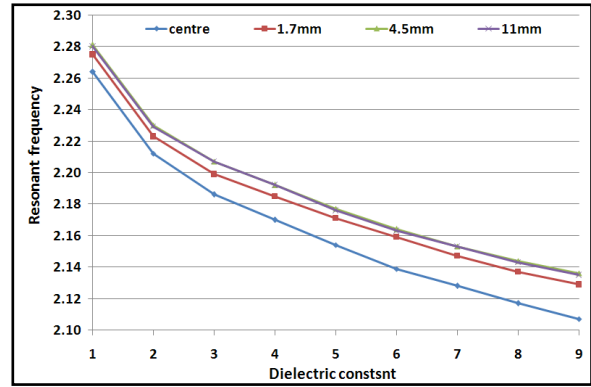


Fig.15.Resonant frequency of sandwich substrate resonator showing the effect of resonator position w.r.t. the centre.

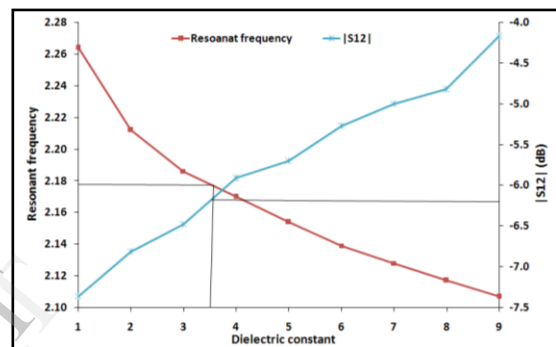


Fig.16.Variation of resonant frequency and $|S_{12}|$ (dB) with dielectric constant of polymer film for resonator placed at the centre (simulation).

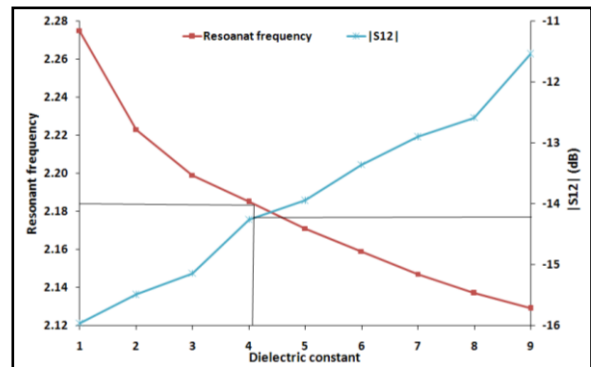


Fig.17.Variation of resonant frequency and $|S_{12}|$ (dB) with dielectric constant of polymer for resonator placed 1.7mm away from centre (simulation).

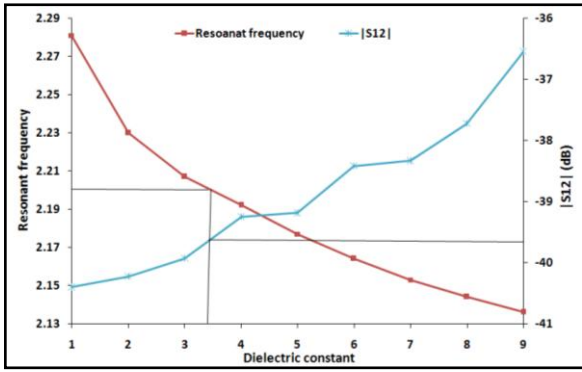


Fig.18.Variation of resonant frequency and $|S_{12}|$ (dB) with dielectric constant of polymer for resonator placed 4.5mm away from centre (simulation).

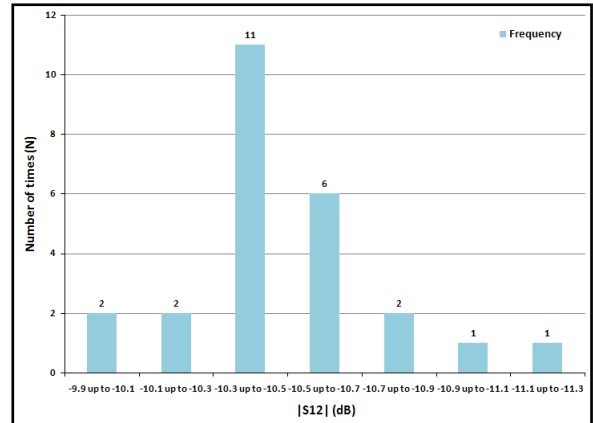


Fig.21.Histogram showing the distribution of measured $|S_{12}|$ (dB) for resonator placed at centre.

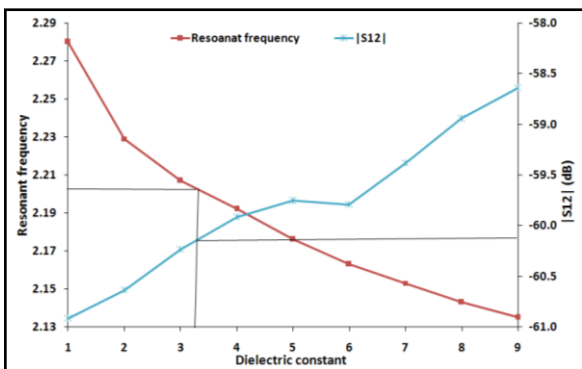


Fig.19.Variation of resonant frequency and $|S_{12}|$ (dB) with dielectric constant of polymer for resonator placed 11mm away from centre (simulation).

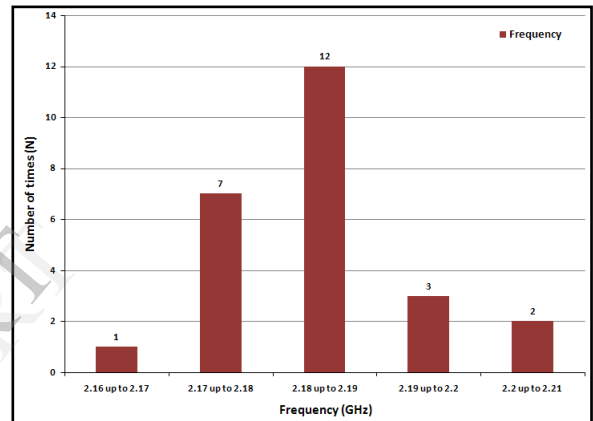


Fig.22. Histogram showing the distribution of measured resonant frequencies for resonator placed 1.7mm away from centre.

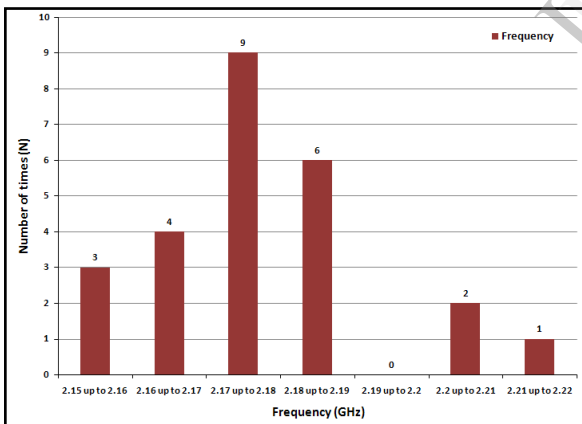


Fig.20.Histogram showing the distribution of measured resonant frequencies for resonator placed at centre.

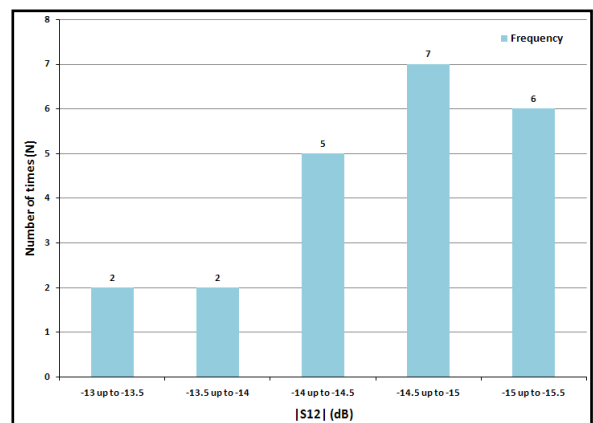


Fig.23.Histogram showing the distribution of measured $|S_{12}|$ (dB) for resonator placed 1.7mm away from centre.

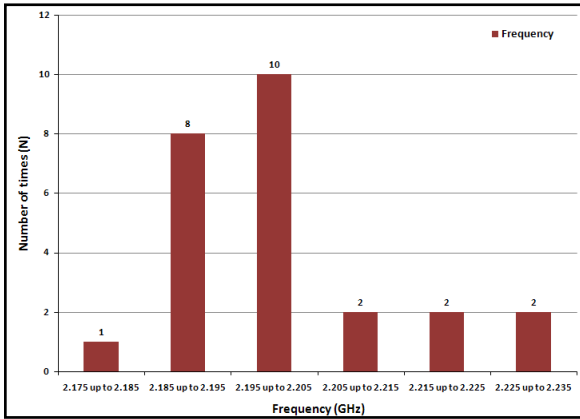


Fig.24. Histogram showing the distribution of measured resonant frequencies for resonator placed 4.5mm away from centre.

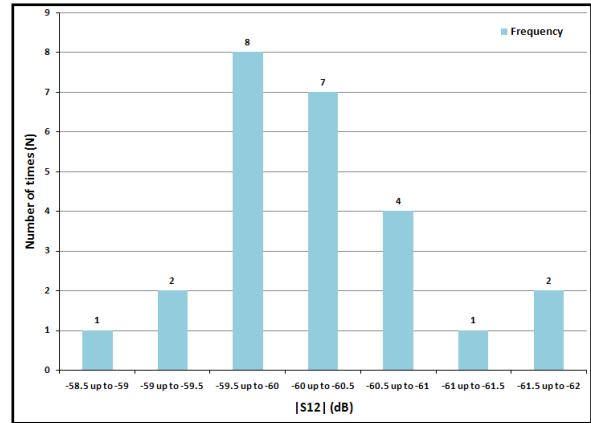


Fig.27. Histogram showing the distribution measured |S₁₂| (dB) for resonator placed 11mm away from centre.

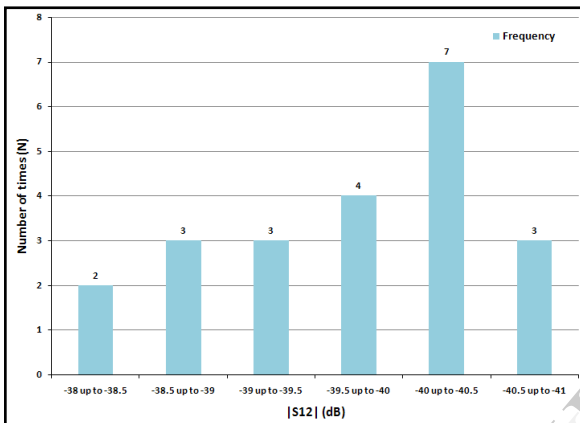


Fig.25. Histogram showing the distribution of measured |S₁₂| (dB) for resonator placed 4.5mm away from centre.

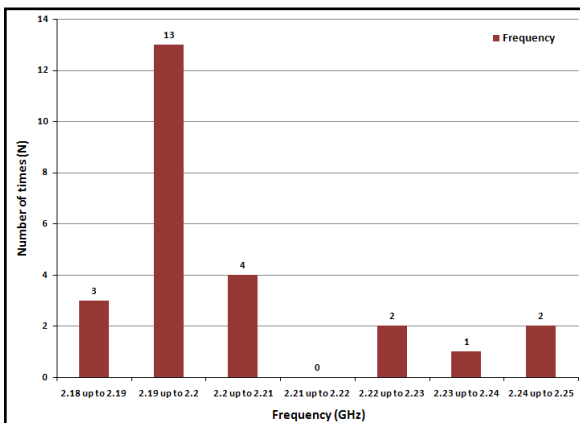


Fig.26. Histogram showing the distribution measured resonant frequencies for resonator placed 11mm away from centre.

We can estimate the permittivity of the polymer from measured resonant frequency and using the data given in

Fig.16 to Fig.19. For example, with no offset, the measured resonant frequency is 2.177 GHz and from

Fig.16, this corresponds to κ lying between 3 and 4. The simulation indicates that |S₁₂| at resonance should be -6.36 dB. However, the measured |S₁₂| is -10.48 dB, which clearly indicates that due to alignment issues, the external loading on resonator is different in simulation and measurement. Thus, this κ is not very reliable.

With the offset of 1.7mm, we get a resonant frequency (measured) of 2.184GHz and from

Fig.17, this corresponds to κ equals to 4. The simulation indicates that |S₁₂| at resonance should be -14.37dB, however, the measured |S₁₂| is -14.75 dB. Thus, this κ is also not very reliable.

With the offset of 4.5 mm, we get a resonant frequency (measured) of 2.201GHz and from

Fig.18 this corresponds to $\kappa=3.5$. For this offset the measured |S₁₂| is -39.93dB and the simulations |S₁₂| is -39.77dB. This indicates that the loading on the resonator is almost same in both simulation and measurement.

Further increasing the offset to 11mm has not changed the resonant frequency but the transmission coefficient has decreased to -60.15 dB. From Fig.19, we find that the simulation gives |S₁₂| of -60.07dB. Thus, using simulations data we can generate calibration curve (like

Fig.18). By knowing the measured resonant frequency, the calibration curve could be used to estimate the permittivity of the polymer. It is important to ensure that the loading on the resonator should be identical both in simulation and measurement. This is achieved by comparing the values of |S₁₂| (dB).

A summary of the measured results, viz, the average and the standard deviation of the resonant frequency and |S₁₂| corresponding to the resonant frequency for four different offsets is given in TABLE 4. When the offset is changed from 4.5mm to 11mm, a very small change in the resonant

frequency is observed. Of course, the $|S_{12}|$ at the resonant frequency decreases considerably, indicating a significant reduction in coupling. A resonant frequency of 2.203GHz corresponds to a permittivity of 3.25.

V. CONCLUSION

In this paper we study the suitability of three types of resonators for estimating the permittivity of the polymer film. Using a half wave microstrip resonator with polymer as an overlay, we observed a change of 102 MHz in the resonant frequency as κ increased from 1 to 9. A microstripring resonator with polymer overlay also showed a decrease in the resonant frequency with increasing κ , but the change was only 93 MHz for $1 \leq \kappa \leq 9$. However, with the polymer forming a sandwich substrate for a microstrip line, we observe 145 MHz change in the resonant frequency for $1 \leq \kappa \leq 9$, even with weak coupling. Thus, the sandwich substrate resonator technique is probably the most accurate method to estimate the permittivity as indicated in TABLE 5.

TABLE 4. SUMMARY OF THE RESULTS FOR SANDWICH SUBSTRATE RESONATOR

Resonator offset (s) (mm)	Frequency (GHz)		$ S_{12} $ (dB)	
	Average	Standard deviation	Average	Standard deviation
0	2.177	0.015	-10.4836	0.2838
1.7	2.184	0.009	-14.7523	0.9179
4.5	2.201	0.013	-39.9318	0.9471
11	2.203	0.016	-60.1581	0.7232

TABLE 5. COMPARISON OF BANDWIDTH OF CHANGE IN RESONANT FREQUENCY WITH PERMITTIVITY FOR DIFFERENT RESONATORS

Resonator	Bandwidth (MHz)
Line resonator	102
Ring resonator	93
Centre	157
1.7mm	146
4.5mm	145
11mm	145

The measurements indicated that, the variability introduced in the placement of the top substrate coupling the microstrip line did affect the measured resonant frequency. In order to understand the nature of error and also improve the accuracy, several measurements had to be carried out, thus limiting the usefulness of the technique.

REFERENCES

- [1] D. A. Rudy, J. P. Mendelsohn and P. J. Muniz, "Measurement of RF dielectric properties with series resonant microstrip elements," *Microwave Journals*, vol. 41, no. 3, pp. 22–41, March 1998.
- [2] P. A. Bernard and J. M. Gautray, "Measurement of dielectric constant using a microstrip ring resonator," *IEEE Transactions on Microwave Theory and Techniques*, vol. 39, no. 3, pp. 592-595, March 1991.
- [3] R. G. Sumesh Sofin and R. C. Aiyer, "Measurement of dielectric constant using a microwave microstrip ring resonator (MMRR) at 10 GHz irrespective of the type of overlay," *Microwave and Optical Technology Letters*, vol. 47, no.1, pp. 11-14, August 2005.
- [4] L. F. Chen, C. K. Ong and C. P. Neo, *Microwave Electronics*, John Wiley & Sons, Ltd, 2004.
- [5] M. Kirschning, R. H. Jansen and N. H. Koster, "Accurate model for open end effect of microstrip lines," *Electronics Letters*, vol. 17, no. 3, pp. 123-125, 1981.
- [6] K. Chang and L. H. Hsieh, *Microwave Ring Circuits and Related Structures*, John Wiley & Sons, Inc., 2004.
- [7] "PCB Impedance and Capacitance Calculator: Embedded Microstrip" http://www.technick.net/public/code/cp_dpage.php?aiocp_dp=util_pcb_imp_microstrip_embed.